Cryptic proteolytic activity of dihydrolipoamide dehydrogenase

Ngolela Esther Babady*†, Yuan-Ping Pang‡, Orly Elpeleg§, and Grazia Isaya*†¶

Departments of *Pediatric and Adolescent Medicine and †Biochemistry and Molecular Biology and ‡Computer-Aided Molecular Design Laboratory, Mayo Clinic College of Medicine, Rochester, MN 55905; and §Metabolic Disease Unit, Hadassah Hebrew University Medical Center, Jerusalem 91120, Israel

Edited by James A. Wells, University of California, San Francisco, CA, and approved February 28, 2007 (received for review November 30, 2006)

The mitochondrial enzyme, dihydrolipoamide dehydrogenase (DLD), is essential for energy metabolism across eukaryotes. Here, conditions known to destabilize the DLD homodimer enabled the mouse, pig, or human enzyme to function as a protease. A catalytic dyad (S456–E431) buried at the homodimer interface was identified. Serine protease inhibitors and an S456A or an E431A point mutation abolished the proteolytic activity, whereas other point mutations at the homodimer interface domain enhanced the proteolytic activity, causing partial or complete loss of DLD activity. In humans, mutations in the DLD homodimer interface have been linked to an atypical form of DLD deficiency. These findings reveal a previously unrecognized mechanism by which certain DLD mutations can simultaneously induce the loss of a primary metabolic activity and the gain of a moonlighting proteolytic activity. The latter could contribute to the metabolic derangement associated with DLD deficiency and represent a target for therapies of this condition.

moonlighting enzymes | protease | mitochondria | frataxin | Friedreich ataxia

Dihydrolipoamide dehydrogenase (DLD) is a flavin-dependent oxidoreductase required for the complete reaction of at least five different multienzyme complexes. In the mitochondrial matrix, the DLD homodimer functions as the E3 component of the pyruvate, α-ketoglutarate, and branched-chain amino acid–dehydrogenase complexes and the glycine cleavage system. In the context of these four multienzyme complexes, DLD utilizes dihydrolipoic acid and NAD^+ to generate lipoic acid and NADH (1). The opposite reaction, from lipoic acid and NADH to dihydrolipoic acid and NAD^+, is catalyzed by the DLD homodimer in the context of the NAD^+-dependent peroxidase–peroxinitrate reductase of *Mycobacterium tuberculosis* (2). In addition, DLD has diaphorase activity, being able to catalyze the oxidation of NADH to NAD^+ by using different electron acceptors such as O_2, labile ferric iron (3), nitric oxide (4), and ubiquinone (5, 6). In this capacity, DLD is believed to primarily have a prooxidant role, achieved by reducing O_2 to a superoxide radical or ferric to ferrous iron, which in turn catalyzes production of hydroxyl radical through Fenton chemistry (3). However, the ability to scavenge nitric oxide and to reduce ubiquinone to ubiquinol suggests that the diaphorase activity of DLD may also have an antioxidant role (4–6). The oligomeric state of DLD can change from dimeric to monomeric or tetrameric depending on the pH in the mitochondrial matrix, and changes in the oligomeric state of the protein have been shown to correlate with a shift from DDL activity (only present in dimeric and tetrameric DLD) to diaphorase activity (present in both oligomeric and monomeric forms of the protein) (7, 8). Thus, DLD represents a highly versatile oxidoreductase with multiple critical roles in energy metabolism and redox balance (2, 7, 9–12).

Here, we found that DLD can also function as a moonlighting protease. Moonlighting enzymes are a growing category of molecules that can accomplish multiple functions through a variety of mechanisms including, among others, localization to different cellular compartments, binding of different cofactors, and changes in oligomerization state (13). Mutations in moonlighting enzymes are predicted to contribute to the phenotypic variability of metabolic disorders (14). In humans, mutations in DLD are linked to a severe disorder of infancy with failure to thrive, hypotonia, and metabolic acidosis, which result from deficient activity of all three α-ketoacid dehydrogenases (15–19). However, the clinical manifestations of DLD deficiency show a great degree of variability (16, 20–23), which has been attributed to varying effects of different DLD mutations on the stability of the protein (20) as well as its ability to dimerize (23, 24) or interact with other components of the three α-ketoacid dehydrogenase complexes (25). Our results suggest a previously unrecognized mechanism by which mutations that alter the stability of the DLD homodimer may not only result in a decrease in the primary metabolic activity of the enzyme but at the same time cause an increase in its moonlighting proteolytic activity. This mechanism is relevant to a complete understanding of the function of DLD and represents a previously unrecognized paradigm for how moonlighting enzymes may influence the complexity of metabolic disorders.

Results

Identification of the Proteolytic Activity of Mouse Liver DLD. The mitochondrial iron chaperone frataxin (26) was used as a substrate to identify proteolytic activities potentially involved in the regulation of mitochondrial iron metabolism. A proteolytic activity that processed the ≈17-kDa mature form of human frataxin (m-fxn) to a product of ≈14 kDa (d-fxn) had been observed in rat liver mitochondria in ref. 27. Here, we detected a similar proteolytic activity in mouse liver mitochondria and isolated it by a three-step chromatographic procedure [supporting information (SI) Table 1]. A fraction with a ≈32,000-fold increase in specific activity was obtained (Mono S fraction; SI Table 1). This fraction catalyzed sequential cleavage of m-fxn to at least four progressively shorter products (denoted d-fxn a, b, c, and d), the smallest of which exhibited an apparent molecular mass of ≈14 kDa (Fig. 1*A*). N-terminal sequencing of the three most abundant products (d-fxn b, c, and d) showed that the proteolytic activity overall removed 21 aa from the N terminus of m-fxn (Fig. 1*B*), with a cleavage specificity partially resembling that of chymotrypsin (C-terminal to F, Y, W, M, or L) (28). An

Author contributions: N.E.B. and G.I. designed research; N.E.B., Y.-P.P., and G.I. performed research; O.E. contributed new reagents/analytic tools; N.E.B., Y.-P.P., and G.I. analyzed data; and N.E.B. and G.I. wrote the paper.

The authors declare no conflict of interest.

This article is a PNAS Direct Submission.

Abbreviations: C-term, homodimer interface domain of human DLD; DFP, diisopropyl fluorophosphate; d-fxn, products derived from cleavage of m-fxn; DLD, dihydrolipoamide dehydrogenase; m-fxn, mature form of human frataxin; MMDS, multiple molecular dynamic simulation.

¶To whom correspondence should be addressed. E-mail: isaya@mayo.edu.

This article contains supporting information online at www.pnas.org/cgi/content/full/0610618104/DC1.

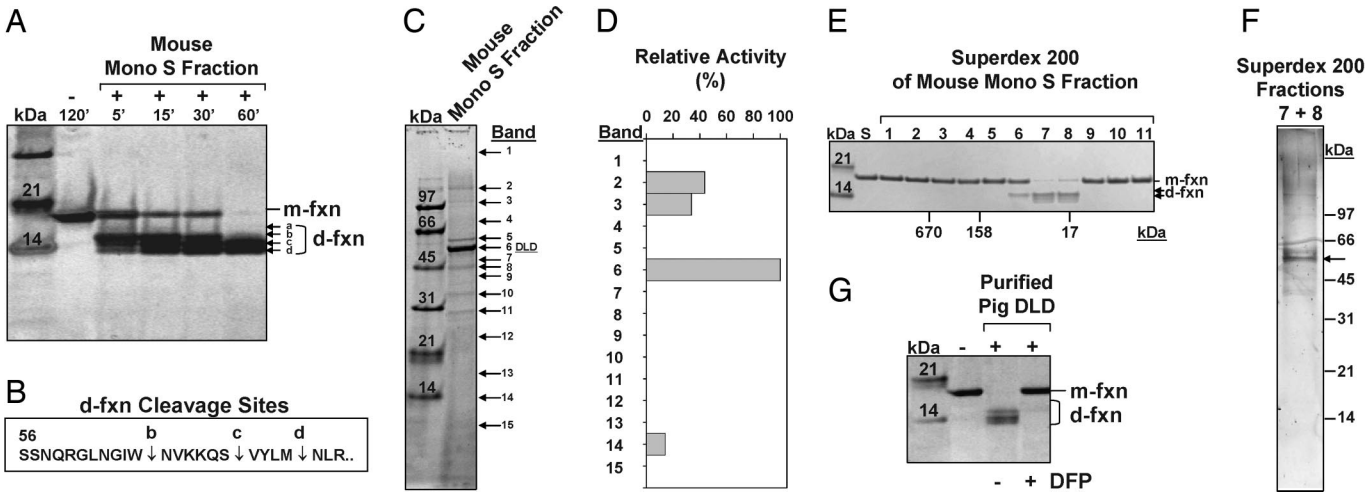

Fig. 1. Identification of mouse DLD as m-fxn degrading activity. (*A*) Time course of cleavage of m-fxn (1.5 μg per lane) in the presence (+) or absence (−) of 1.5 μg (total protein) of mouse liver Mono S fraction. Each reaction was incubated at 37°C in 10 mM Tris·HCl, pH 8.0, for the indicated time and analyzed by SDS/12% PAGE and SYPRO orange staining. (*B*) Cleavage sites in m-fxn substrate were determined by subjecting the d-fxn b, c, and d products to N-terminal sequencing. (*C*) Mouse Mono S fraction (3 μg of total protein) analyzed by SDS/12% PAGE and silver staining. (*D*) All visible protein bands (numbered 1 to 15) were excised from the gel in *C*, and each gel slice was extracted in 20 μl of 10 mM Tris·HCl, pH 8.0, and 1% Triton X-100 and assayed for proteolytic activity for 24 h. Activity was expressed as percent of the total activity recovered in band 6, which was identified as mouse DLD by MS. The DLD protein was also detected by MS in bands 2 and 3 (see *Results*). Results presented below suggest that a proteolytically active ≈14 kDa fragment of DLD was present in band 14. (*E*) An aliquot (≈25 μg of total protein) of mouse Mono S fraction was loaded on a Superdex 200 column (10 mm × 30 cm). Aliquots of fractions 1–11, comprising the void volume and the entire molecular mass range of the column (10–600 kDa), were analyzed for m-fxn-degrading activity as in Fig. 1 *A*. S, reaction containing m-fxn substrate only. (*F*) Because of the limited amount of starting material, DLD or other proteins could not be detected by SDS/PAGE in aliquots from the Superdex 200 fractions described above. Therefore, active fractions 7 and 8 were pooled and concentrated, and total protein was precipitated with 10% trichloroacetic acid and analyzed by SDS/PAGE and silver staining. The arrow points at the ≈50-kDa DLD band, as determined in Fig. 1*C*. (*G*) A commercial preparation of pig heart DLD (L2002; Sigma, St. Louis, MO) was purified through Mono S, hydroxyapatite, and Superdex 200 chromatography, as described in SI Fig. 7 *C–E*. The purest fraction obtained (fraction 7 + 8 in SI Fig. 7*E*) was preincubated for 1 h with (+) or without (−) 1 mM DFP, an irreversible serine protease inhibitor, in 10 mM Hepes-KOH, pH 6.8, 100 mM NaCl, and 0.1% Triton X-100 [proteolytic reaction buffer (PRB)] at 37°C; m-fxn substrate was added, and activity was assayed for 2 h.

aliquot of the Mono S fraction was digested in solution with trypsin and analyzed by nano-liquid chromatography/tandem MS (nanoLC-MS/MS) at the Mayo Proteomics Research Center (Mayo Clinic, Rochester, MN). This method can detect both high- and low-abundance proteins in a complex mixture with sensitivity in the low femtomole range (29). Mascot (Matrix Sciences, London, U.K.) (30) was used to match the MS/MS spectra against the proteins in the Swissprot database. Several mostly mitochondrial proteins, but no known proteases, were present in the Mono S fraction (data not shown). As analyzed by SDS/PAGE and silver staining, the Mono S fraction contained a predominant protein band of ≈50 kDa, which was not present in inactive fractions, and several additional protein bands (Fig. 1*C* and SI Fig. 5 *A* and *B*). All visible proteins were eluted from the gel by passive diffusion (31) (Fig. 1*C*, bands 1–15) and tested for proteolytic activity with m-fxn (Fig. 1*D*). The proteolytic activity was primarily associated with the ≈50-kDa band (Fig. 1 *C* and *D*, band 6), although lower levels of activity were found in two gel slices >97 kDa and one at ≈14 kDa (Fig. 1 *C* and *D*, bands 2, 3, and 14). In-gel trypsin digestion, nanoLC-MS/MS, and Mascot analysis of the ≈50-kDa band yielded several peptides that matched the sequence of mouse DLD (64% coverage) and no other significant hits. The two active bands >97 kDa cross-reacted with a polyclonal anti-DLD antibody and were present both in the mouse Mono S fraction and in a commercial preparation of pig heart DLD (SI Fig. 6). In-gel trypsin digestion, nanoLC-MS/MS, and Mascot analysis of these bands from the mouse Mono S fraction or the pig DLD preparation yielded several DLD peptides (13% and 59% coverage, respectively), suggesting that unresolved DLD dimers were present in this region of the gel. This procedure was not attempted on band 14 because of insufficient protein levels. However, deletion mutagenesis of DLD later suggested that the 14-kDa region of the gel probably contained a proteolytically active C-terminal fragment of the protein (see below). The ≈50-kDa band continued to represent the main species detected in proteolytically active fractions upon Superdex 200 (GE Healthcare, Little Chalfont, U.K.) gel filtration of the mouse Mono S fraction (Fig. 1 *E* and *F*). Thus, the proteolytic activity appeared to be consistently associated with the presence of the DLD protein.

Proteolytic Activity of Pig Heart DLD. Next, we investigated whether a commercial preparation of pig heart DLD exhibited proteolytic activity. As analyzed by SDS/PAGE and protein staining with SYPRO orange, this DLD preparation was >90% pure (SI Fig. 7*A*). It exhibited DLD activity (data not shown) but was proteolytically inactive against m-fxn (SI Fig. 7*B*). The total m-fxn degrading activity purified from mouse liver mitochondria had also been low at the end of the first chromatographic step (Uno Q; Bio-Rad, Hercules, CA) but had consistently increased by nearly 8-fold after the second step (hydroxyapatite; SI Table 1). Similarly, when the pig DLD preparation was subjected to hydroxyapatite chromatography, weak but clear proteolytic activity was associated with the DLD protein (SI Fig. 7*C*), and the activity continued to be associated with pig DLD upon additional purification steps (SI Fig. 7 *D* and *E*) as observed with mouse DLD (Fig. 1 *E* and *F*). The purified pig DLD preparation was subjected to trypsin digestion, nano-liquid chromatography/tandem MS (nanoLC-MS/MS), and Mascot search. Only two proteins were present in addition to DLD; these proteins were different from the proteins identified in the mouse Mono S fraction (data not shown) and once again did not include any known protease (SI Table 2).

Proteolytic Activity of Recombinant Human DLD. The DLD dimer is in a dynamic equilibrium with the monomer; the equilibrium can

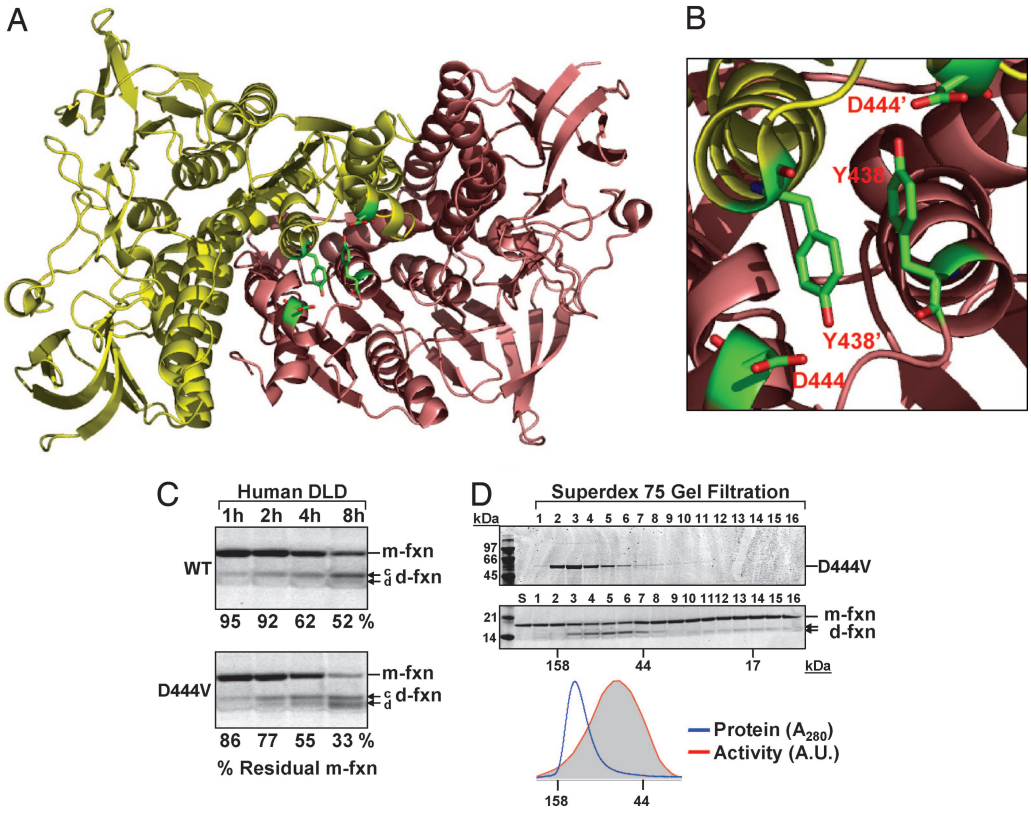

Fig. 2. D444V mutation in the human DLD homodimer interface increases DLD proteolytic activity. (*A* and *B*) The two subunits of the human DLD homodimer (1ZMC) (36) are shown in ribbon representation, with the D444 and Y438 residues shown as sticks. Figures generated with PyMOL. (*C*) Time courses of proteolytic activity were performed with purified recombinant human WT or D444V DLD (5 μg per reaction) in proteolytic reaction buffer (PRB) with 1 μg per reaction of m-fxn substrate and were analyzed by SDS/PAGE and SYPRO orange staining. The percent residual m-fxn was determined by densitometry; values at the bottom of each blot represent the average of two independent experiments, one of which is shown. SDS/PAGE analysis of WT and D444V DLD is shown in SI Fig. 8*A*. (*D*) Purified D444V DLD (1.5 mg) was fractionated on a Superdex 75 gel filtration column. (*Top* and *Middle*) Ten microliters from each fraction were used to detect DLD protein (*Top*) or measure proteolytic activity (*Middle*). (*Bottom*) The graph shows the protein elution profile (blue) superimposed to that of the proteolytic activity (red), which was quantified by densitometry. A.U., arbitrary units.

be shifted toward monomer by freezing–thawing, high salt concentrations, protein dilution, and other conditions (32–34). Activation of DLD proteolytic activity by high salt concentrations was observed during hydroxyapatite fractionation of the mouse DLD (SI Table 1) and pig DLD (SI Fig. 7*C*) preparations, and freezing–thawing resulted in further activation of both enzymes (SI Fig. 7*E* and data not shown). Conversely, both mouse and pig DLD were fully inactivated by 1 mM diisopropyl fluorophosphate (DFP), an irreversible serine protease inhibitor (35) (Fig. 1*G* and data not shown). From these observations, we hypothesized that destabilization of the DLD homodimer might enable the enzyme to function as a serine protease.

In humans, DLD mutations that affect the DLD activity are linked to a severe metabolic disorder (23). We analyzed a pathogenic mutation (D444V) in the DLD homodimer interface previously hypothesized to result in loss of DLD activity by perturbing the stability of the homodimer (24). The D444V mutation causes the loss of two symmetric hydrogen bonds that normally form between residue D444 of one subunit and residue Y438 of the opposite subunit (36) (Fig. 2 *A* and *B*). Patients homozygous for the D444V mutation exhibit a drastic reduction in DLD protein levels and a parallel loss of DLD activity (13% and 15% of controls, respectively) (24). A total cell extract from a previously characterized fibroblast cell line from a patient homozygous for the D444V mutation (24) showed decreased levels of DLD protein but more efficient cleavage of m-fxn substrate to d-fxn relative to a control cell line (data not shown), suggesting that the proteolytic activity of human DLD was enhanced by the D444V mutation. To confirm this observation, the WT human DLD (WT DLD) and the D444V variant (D444V DLD) were expressed in *Escherichia coli* with an N-terminal six-histidine tag and purified in one step by nickel affinity chromatography (SI Fig. 8*A*). This procedure, which was completely different from those used for mouse or pig DLD, yielded DLD and trace amounts of a handful of *E. coli* proteins, different from the proteins identified in the mouse or pig DLD preparations (*SI Methods* and SI Tables 2 and 3). Both WT and D444V DLD exhibited weak proteolytic activity with m-fxn substrate; however, D444V DLD consistently cleaved m-fxn to d-fxn products with faster kinetics than WT DLD (Fig. 2*C*). When DLD D444V was subjected to gel filtration, the bulk of the DLD protein was eluted with the molecular mass of the dimer, ≈100 kDa (Fig. 2*D Top*, fractions 2–4). However, lower protein levels were eluted with a molecular mass consistent with that of DLD monomer, ≈50 kDa (Fig. 2*D Top*, fractions 5–7). The proteolytic activity peaked within these fractions (Fig. 2*D Middle*, fractions 5 and 6). Similarly, when the mouse or pig DLD preparations were analyzed by Superdex 200 gel filtration, low DLD protein levels were detected in the most active fractions (Fig. 1 *E* and *F*, fractions 7 and 8, and SI Fig. 7*E*, fractions 7 and 8) with a molecular mass consistent with that of the DLD monomer. These data suggest that the proteolytic activity of DLD is induced by conditions that destabilize the DLD homodimer.

Characterization of DLD Proteolytic Activity. The proteolytic activities of the native mouse and pig DLDs and recombinant human

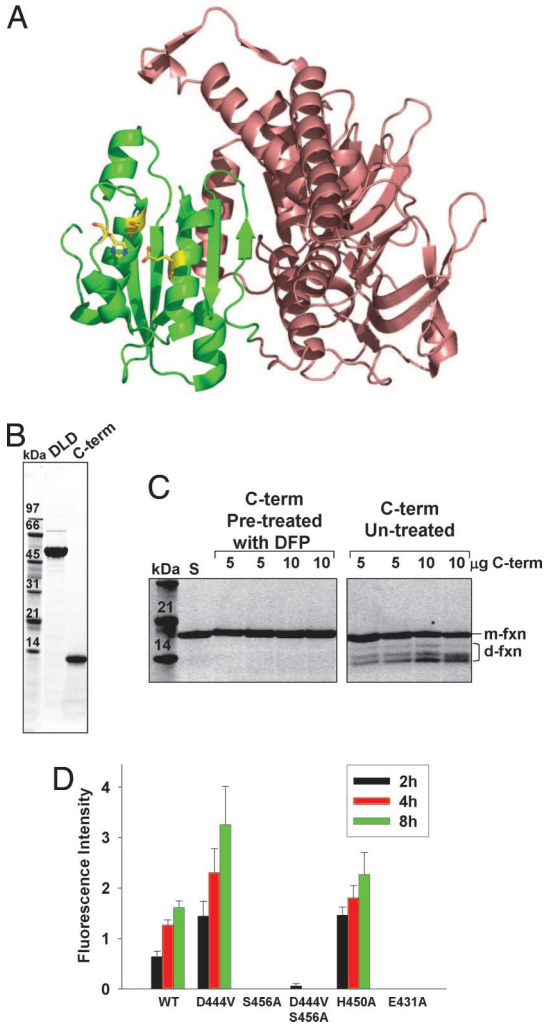

Fig. 3. Identification of serine protease active-site residues at the DLD homodimer interface. (*A*) One subunit of human DLD homodimer (1ZMC) is shown in ribbon representation with the dimer interface domain (residues 350–474) in green, and residues S456, H450, and E431 are shown as sticks. The figure created with PyMOL. (*B*) The C-term, corresponding to the dimer interface domain, was expressed in *E. coli* and purified (*SI Methods* and SI Table 4). C-term (5 μg) was analyzed by SDS/12% PAGE and SYPRO orange staining alongside the full-length human DLD. (*C*) Aliquots (5 or 10 μg) of C-term DLD were incubated with or without 1 mM diisopropyl fluorophosphate or phosphorofluoridate (DFP) in duplicate for 24 h at 37°C. All protein samples were resolved on SDS/12% PAGE, visualized by silver staining, eluted from gel slices by passive diffusion, and tested for proteolytic activity with m-fxn substrate as described in Fig. 1 *C* and *D*. Shown are the results obtained with eight independent gel slices. (*D*) WT and mutant DLD proteins were purified at the same time and assayed simultaneously in a 96-well plate by using a fluorogenic peptide substrate consisting of 13 aa from the m-fxn N-terminal region, with a fluorescent donor and a quenching acceptor (*see Experimental Methods*). Each reaction contained 2 μM DLD and 50 μM peptide in 100 μl of 10 mM Tris·HCl, pH 8.0, and 50 mM NaCl. Total fluorescence was measured after 2, 4, and 8 h of incubation at 37°C. Blanks containing DLD protein only or substrate only in buffer were run in parallel with proteolytic reactions. Bars represent fluorescence intensity after background subtraction. Each bar represents the mean ± SE of three (WT and D444V) or two (S456A, S456A/D444V, E431A, and H450A) independent experiments, each conducted in duplicate. SDS/PAGE analysis of all proteins is shown in SI Fig. 8*A*.

DLD were consistently inhibited by certain serine protease inhibitors, whereas inhibitors of other classes of proteases had inconsistent effects (Fig. 1*G* and data not shown). Kinetic constants were determined for D444V DLD by using the chromogenic serine hydrolase substrate *p*-nitrophenyl butyrate (pNPB) (37). D444V DLD hydrolyzed pNPB in a protein concentration-dependent manner (SI Fig. 9*A* and *SI Methods*) with a V_{max} of 3,085 nM/min and a K_m of 1.36 mM (SI Fig. 9 *B* and *D*), and was inhibited by DFP with an IC_{50} of 1.96 μM (SI Fig. 9 *C* and *D*). In Fig. 1 *C* and *D*, we had detected some proteolytic activity in a region of the gel corresponding to ≈14 kDa. Similarly, when human D444V DLD had been subjected to gel filtration, low levels of activity were present in fractions with a molecular mass close to 14 kDa (Fig. 2*D*, fractions 12–15). We further noted that the interface domain of the DLD homodimer encompasses the 126 C-terminal residues of the protein (C-term) (Fig. 3*A*) with a calculated molecular mass of 13,551 Da, suggesting that the proteolytic activity of DLD might reside in the interface domain. Therefore, this domain was expressed in *E. coli* without any tags and purified to near homogeneity by a five-step procedure (Fig. 3*B*, *SI Methods*, and SI Table 4). Purified C-term DLD was run on a SDS/12% PAGE gel, eluted from gel slices by passive diffusion, and tested for proteolytic activity with m-fxn as described in Fig. 1 *C* and *D*. We observed m-fxn cleavage, which was proportional to the amounts of C-term protein present in each gel slice (Fig. 3*C*). The activity was fully inhibited when C-term protein was treated with the covalent serine protease inhibitor, DFP, before SDS/PAGE (Fig. 3*C*). C-term DLD was also active against pNPB and a fluorogenic peptide (data not shown).

Identification of a Putative Serine Catalytic Dyad in DLD Monomer. A sequence analysis of DLD did not identify any of the classic serine protease motifs (38), however, visual inspection of the crystal structure of human DLD homodimer revealed three residues (S456–H450–E431) that might form a serine catalytic triad at the homodimer interface, according to distance criteria (Fig. 3*A*). Full-length DLD proteins with point mutations in these residues were expressed in *E. coli* and purified by affinity chromatography. WT and mutant DLD proteins exhibited very similar expression levels and purification yields. They also displayed a very similar degree of purity (SI Fig. 8*A*) but different levels of proteolytic activity (Fig. 3*D*). Alanine replacement of S456 or E431 resulted in a complete loss of proteolytic activity as measured with a fluorogenic peptide encompassing the m-fxn N-terminal region (Fig. 3*D*). A double mutation, S456A/D444V, gave low levels of residual activity (Fig. 3*D*, 2 h). Other studies have shown that removal of the catalytic serine does not always completely abolish the proteolytic activity of serine proteases, either because a water molecule can serve as a "spare tire" for the hydroxyl group of the catalytic serine or because binding and orientation of the substrate is sufficient for a small amount of catalysis (39, 40). Either mechanism may have been slightly favored in the presence of the D444V mutation, resulting in the low levels of activity detected at 2 h with the D444V/S456A DLD protein. Unlike the activity of WT or D444V DLD, however, the residual activity of D444V/S456A DLD did not increase over time and was lower than the background fluorescence at 4 and 8 h (Fig. 3*D*).

In contrast to S456 or E431, alanine replacement of H450 resulted in an increase in proteolytic activity as compared with WT DLD (Fig. 3*D*). In an effort to explain this result, multiple molecular dynamic simulations (MMDSs) (10 ns for each simulation with a 1.0-fs time step and different initial velocities; 100 simulations for each protein; see *SI Methods*) were performed on the monomeric C-term domain of WT DLD and H450A DLD by using a published protocol (39). An MMDS-refined model of monomeric WT C-term domain shows that the carboxylate group of E431 forms hydrogen bonds with both the hydroxyl group of S456 and the imidazole group of H450 (Fig. 4*A*), whereas E431 does not have a hydrogen bond to S456 in the crystal structure of human DLD homodimer. This finding suggests that S456 and E431 form a catalytic dyad in

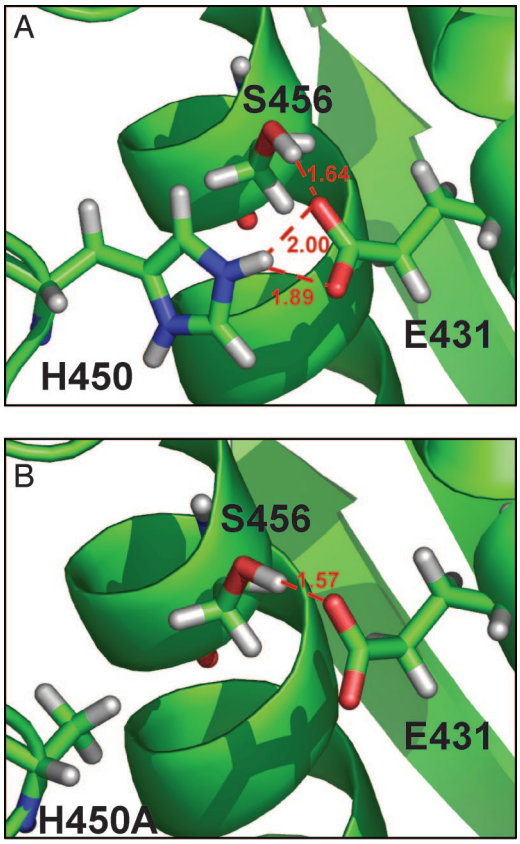

Fig. 4. Putative catalytic dyad at the DLD homodimer interface domain. Models of monomeric WT (*A*) and H450A (*B*) DLD homodimer interface domain (residues 350–474; C-term) obtained by MMDSs (39). Close-ups of the putative S456–E431 dyad were generated with PyMOL.

the DLD monomer, and that H450, by forming a hydrogen bond with E431, may decrease the ability of E431 to polarize the hydroxyl group of S456. Indeed, an MMDS-refined model of monomeric H450A C-term domain shows that the H450A mutation abolishes the hydrogen bond between E431 and H450, consequently strengthening the hydrogen bond between E431 and S456 (Fig. 4*B*). This may increase the polarization of the S456 hydroxyl group, explaining the higher proteolytic activity observed with H450A DLD relative to WT DLD (Fig. 3*D*).

All MMDSs did not identify any other residues in the monomeric C-term domain with a spatial position suitable to serve as the general base, as found in canonical serine catalytic triads. The putative S456-E431 dyad in the MMDS-refined models is located in what appears as a possible peptide-binding pocket (Fig. 10*A*) and could function similarly to the Ser–Asp dyad of phospholipase A (41, 42) or the Ser–Glu dyad of β-lactamases (43), which are thought to use a nucleophilic serine and a carboxylate residue that acts as a proton acceptor. The presence of a dyad may explain the slow enzyme kinetics measured with *p*-nitrophenyl butyrate (pNPB) and D444V DLD (SI Fig. 9) as compared, for example, with subtilisin (37), which uses a classic triad. Both S456 and E431 are conserved in all known eukaryotic and some prokaryotic DLD sequences, but not other members of the pyridine nucleotide disulfide oxidoreductases (SI Fig. 10*B*) (44), suggesting that the proteolytic activity is a specific function of DLD.

Interestingly, the mutations described above had variable effects on the DLD activity (SI Fig. 8*B*). In particular, one proteolytically inactive protein, S456A DLD, exhibited normal dehydrogenase activity, whereas D444V or H450A DLD, which had higher proteolytic activity than WT DLD, exhibited partial or nearly complete loss of dehydrogenase activity (SI Fig. 8*B*), suggesting that the two activities of DLD may be independently modulated.

Discussion

Moonlighting proteins represent a growing class of molecules that perform two or more different functions (13, 45). These proteins are thought to have evolved because they can provide cells with significant advantages, namely, the ability to increase the spectrum of metabolic activities without increasing the number of protein-coding genes, and the ability to coordinate different metabolic pathways (13). A previously unrecognized moonlighting mechanism emerges from our findings. The moonlighting proteolytic activity of DLD is revealed by conditions that destabilize the DLD homodimer and decrease to various degrees its DLD activity. Interestingly, a recent study has shown that acidification of the mitochondrial matrix, as it occurs during ischemia-reperfusion injury, disrupts the quaternary structure of DLD, leading to a decrease in dehydrogenase activity and an increase in diaphorase activity (7). The latter is an FAD- and NADH-dependent activity believed to mainly have a prooxidant role (3). These findings together suggest that, under physiological conditions, DLD primarily functions as a DLD, playing a central role in the maintenance of energy metabolism (9–12). Conversely, the moonlighting proteolytic activity of DLD could arise under pathological conditions, including the presence of dimer-destabilizing mutations or the acidification of the mitochondrial matrix (7). In such conditions, a reduction in energy metabolism (due to the loss of DLD activity) and an increase in oxidative damage (due to increased diaphorase activity) (7) could be further complicated by the appearance of proteolytic activity. Proteolytically active DLD removes a functionally critical domain from the N terminus of frataxin, a mitochondrial protein involved in iron metabolism and antioxidant protection (26, 46), deficiency of which is responsible for the neurodegenerative and cardiac disease Friedreich ataxia (47). If frataxin and/or other mitochondrial proteins are the natural substrates of proteolytically active DLD, then the presence or absence of this accessory activity could greatly influence cell survival during ischemia-reperfusion injury as well as affect the biochemical consequences of genetically determined DLD deficiency. It has been proposed that moonlighting proteins can enhance the phenotypic variability of single-gene disorders (14). In this respect, it is noteworthy that patients with point mutations at the DLD homodimer interface (D444V or R447G) were affected with hypertrophic cardiomyopathy, which is one of the manifestations of Friedreich ataxia (47) and has not been observed in association with other DLD mutations (23). Conversely, partial DLD deficiency was observed in a subset of Friedreich ataxia patients (48, 49). Our findings should lead to future studies to assess how the moonlighting proteolytic activity of DLD contributes to the phenotypic manifestations of DLD deficiency, Friedreich ataxia, and ischemia reperfusion injury, and whether it could represent a target for therapies of these conditions.

Experimental Methods

Proteolytic Activity Assays. The m-fxn substrate corresponds to the mature form of human frataxin (residues 56–210, i.e., lacking the mitochondrial matrix targeting signal) (27), which was produced in *E. coli* and purified as described in ref. 46. Proteolytic activity was measured by the conversion of m-fxn to d-fxn products for the indicated periods of time at 37°C as analyzed by SDS/PAGE and protein staining. For a fluorescence-based assay, a peptide encompassing cleavage sites c and d in the m-fxn N terminus (Fig. 1*B*) was custom-made by AnaSpec (San Jose, CA). The peptide consists of 13 aa residues (NH_2-K-K-E[EDANS]S-V-Y-L-M-N-L-R-K[DAB-

CYL]-S-NH_2) with a fluorescent donor, 5-[(2-aminoethyl) amino] naphtalene-1-sulfonic acid (EDANS), and a quenching acceptor, 4-(4-dimethyl-aminophenylazo) benzoic acid (DABCYL) (50). The assay was carried out in 96-well plates (Corning Costar, Corning, NY) in a Fluoroskan Ascent fluorometer (Thermo Electron, San Jose, CA) with excitation and emission wavelengths of 355 and 495 nm, respectively. Additional details are available in the figure legends and in *SI Methods*.

Detailed descriptions of all materials and methods are provided in *SI Methods*.

We thank Dr. D. Danner (Emory University, Atlanta, GA) for the human DLD cDNA; Dr. D. Oglesbee (Mayo Clinic College of Medicine) for assistance with cell cultures; Dr. O. Gakh (Mayo Clinic College of Medicine) for helpful discussions; Dr. B. Madden (Mayo Proteomic Research Center, Rochester, MN) for MS data; and D. Smith for excellent technical assistance. This work was supported by a Muscular Dystrophy Association grant (to G.I.), American Heart Association Grants 065007Z (to G.I.) and 0415379Z (to N.E.B.), Defense Advanced Research Projects Agency Grant DAAD19-01-1-0322 (to Y.-P.P.), and U.S. Army Medical Research Aquisition Activity Grant W81XWH-04-2-0001 (to Y.-P.P.).

1. Carothers DJ, Pons G, Patel MS (1989) *Arch Biochem Biophys* 268:409–425.
2. Bryk R, Lima CD, Erdjument-Bromage H, Tempst P, Nathan C (2002) *Science* 295:1073–1077.
3. Petrat F, Paluch S, Dogruoz E, Dorfler P, Kirsch M, Korth HG, Sustmann R, de Groot H (2003) *J Biol Chem* 278:46403–46413.
4. Igamberdiev AU, Bykova NV, Ens W, Hill RD (2004) *FEBS Lett* 568:146–150.
5. Olsson JM, Xia L, Eriksson LC, Bjornstedt M (1999) *FEBS Lett* 448:190–192.
6. Xia L, Bjornstedt M, Nordman T, Eriksson LC, Olsson JM (2001) *Eur J Biochem* 268:1486–1490.
7. Klyachko NL, Shchedrina VA, Efimov AV, Kazakov SV, Gazaryan IG, Kristal BS, Brown AM (2005) *J Biol Chem* 280:16106–16114.
8. Tsai CS, Templeton DM, Wand AJ (1981) *Arch Biochem Biophys* 206:77–86.
9. Chuang DT, Shih VE (2001) in *The Metabolic & Molecular Bases of Inherited Disease*, eds Scriver C, Beaudet AL, Sly WS, Valle D (McGraw–Hill, New York), pp 1971–2005.
10. Goodman SI, Frerman FE (2001) in *The Metabolic & Molecular Bases of Inherited Disease*, eds Scriver C, Beaudet AL, Sly WS, Valle D (McGraw-Hill, New York), pp 2195–2204.
11. Munnich A, Saudubray JM, Taylor J, Charpentier C, Marsac C, Rocchiccioli F, Amedee-Manesme O, Coude FX, Frezal J, Robinson BH (1982) *Acta Paediatr Scand* 71:167–171.
12. Robinson BH (2001) in *The Metabolic & Molecular Bases of Inherited Disease*, eds Scriver C, Beaudet AL, Sly WS, Valle D (McGraw–Hill, New York), pp 2275–2295.
13. Jeffery CJ (1999) *Trends Biochem Sci* 24:8–11.
14. Sriram G, Martinez JA, McCabe ER, Liao JC, Dipple KM (2005) *Am J Hum Genet* 76:911–924.
15. Craigen WJ (1996) *Pediatr Neurol* 14:69–71.
16. Elpeleg ON, Shaag A, Glustein JZ, Anikster Y, Joseph A, Saada A (1997) *Hum Mutat* 10:256–257.
17. Elpeleg ON, Saada AB, Shaag A, Glustein JZ, Ruitenbeek W, Tein I, Halevy J (1997) *Muscle Nerve* 20:238–240.
18. Aptowitzer I, Saada A, Faber J, Kleid D, Elpeleg ON (1997) *J Pediatr Gastroenterol Nutr* 24:599–601.
19. Robinson BH, Sherwood WG, Kahler S, O'Flynn ME, Nadler H (1981) *N Engl J Med* 304:53–54.
20. Shaag A, Saada A, Berger I, Mandel H, Joseph A, Feigenbaum A, Elpeleg ON (1999) *Am J Med Genet* 82:177–182.
21. Grafakou O, Oexle K, van den Heuvel L, Smeets R, Trijbels F, Goebel HH, Bosshard N, Superti-Furga A, Steinmann B, Smeitink J (2003) *Eur J Pediatr* 162:714–718.
22. Cerna L, Wenchich L, Hansikova H, Kmoch S, Peskova K, Chrastina P, Brynda J, Zeman J (2001) *Med Sci Monit* 7:1319–1325.
23. Odievre MH, Chretien D, Munnich A, Robinson BH, Dumoulin R, Masmoudi S, Kadhom N, Rotig A, Rustin P, Bonnefont JP (2005) *Hum Mutat* 25:323–324.
24. Shany E, Saada A, Landau D, Shaag A, Hershkovitz E, Elpeleg ON (1999) *Biochem Biophys Res Commun* 262:163–166.
25. Brautigam CA, Wynn RM, Chuang JL, Machius M, Tomchick DR, Chuang DT (2006) *Structure (London)* 14:611–621.
26. Al-Karadaghi S, Franco R, Hansson M, Shelnutt JA, Isaya G, Ferreira GC (2006) *Trends Biochem Sci* 31:135–142.
27. Cavadini P, Adamec J, Taroni F, Gakh O, Isaya G (2000) *J Biol Chem* 275:41469–41475.
28. Keil B (1987) *Protein Seq Data Anal* 1:13–20.
29. Wu CC, MacCoss MJ (2002) *Curr Opin Mol Ther* 4:242–250.
30. Perkins DN, Pappin DJ, Creasy DM, Cottrell JS (1999) *Electrophoresis* 20:3551–3567.
31. Jeohn GH, Matsuzaki H, Takahashi K (1999) *Eur J Biochem* 260:318–324.
32. v Muiswinkel-Voetberg H, Visser J, Veeger C (1973) *Eur J Biochem* 33:265–270.
33. van Berkel WJ, Benen JA, Snoek MC (1991) *Eur J Biochem* 197:769–779.
34. Visser J, McCormick DB, Veeger C (1968) *Biochim Biophys Acta* 159:257–264.
35. Powers JC, Harper JW (1986) in *Proteinases Inhibitors*, eds Barret AJ, Salvesen G (Elsevier Sciences, Amsterdam), pp 55–152.
36. Brautigam CA, Chuang JL, Tomchick DR, Machius M, Chuang DT (2005) *J Mol Biol* 350:543–552.
37. Philipp M, Tsai IH, Bender ML (1979) *Biochemistry* 18:3769–3773.
38. Rawlings ND, Morton FR, Barrett AJ (2006) *Nucleic Acids Res* 34:D270–D272.
39. Pang YP (2004) *Proteins* 57:747–757.
40. Peracchi A (2001) *Trends Biochem Sci* 26:497–503.
41. Hirschberg HJ, Simons JW, Dekker N, Egmond MR (2001) *Eur J Biochem* 268:5037–5044.
42. Dessen A, Tang J, Schmidt H, Stahl M, Clark JD, Seehra J, Somers WS (1999) *Cell* 97:349–360.
43. Damblon C, Raquet X, Lian LY, Lamotte-Brasseur J, Fonze E, Charlier P, Roberts GC, Frere JM (1996) *Proc Natl Acad Sci USA* 93:1747–1752.
44. Williams CHJ (1992) in *Chemistry and Biochemistry of Flavoenzymes*, ed Muller F (CRC, Boca Raton FL), pp 121–212.
45. Khersonsky O, Roodveldt C, Tawfik DS (2006) *Curr Opin Chem Biol* 10:498–508.
46. O'Neill HA, Gakh O, Park S, Cui J, Mooney SM, Sampson M, Ferreira GC, Isaya G (2005) *Biochemistry* 44:537–545.
47. Campuzano V, Montermini L, Molto MD, Pianese L, Cossee M, Cavalcanti F, Monros E, Rodius F, Duclos F, Monticelli A, *et al.* (1996) *Science* 271:1423–1427.
48. Kark RA, Budelli MM, Becker DM, Weiner LP, Forsythe AB (1981) *Neurology* 31:199–202.
49. Mastrogiacomo F, LaMarche J, Dozic S, Lindsay G, Bettendorff L, Robitaille Y, Schut L, Kish SJ (1996) *Neurodegeneration* 5:27–33.
50. Matayoshi ED, Wang GT, Krafft GA, Erickson J (1990) *Science* 247:954–958.